

# Numerical Study of Stress Distribution in Soft Clay Treated with Stone Column

Maki J. M. Al-Waily<sup>1, a \*</sup> and Maysa S. Al-Qaisi<sup>1, b</sup>

<sup>1</sup>AL-Musaib Technical College, Al-Furat Al-Awsat Technical University, Kufa, Iraq.

<sup>a</sup>[maki\\_jafar@atu.edu.iq](mailto:maki_jafar@atu.edu.iq) and <sup>b</sup>[maysasalem@atu.edu.iq](mailto:maysasalem@atu.edu.iq)

\*Corresponding author

**Abstract.** This study used a finite element analysis approach employing Plaxis 3D to analyze the stress concentration ratio, a critical parameter in geotechnical engineering, to examine stresses operating on stone columns and soft soils. This study also looked at the effect of the stiffness ratio between the stone column and the neighboring soil. With the same length and three different diameters, 0.8 m, 1.0 m, and 1.2 m, or three area replacement ratios ranging from 7% to 16%, respectively, floating and end-bearing stone columns were used. The influence of soft soil undrained cohesion,  $c_u$  ranging from 6 kPa to 40 kPa, was also considered in the current study. The stiffness ratio for columns to adjacent soil, end bearing or floating stone column, and area ratio all have a significant impression on the performance of the stone column in treating soft soil and stress transmission mechanisms in the enhanced soil body, according to parametric studies. The average stress concentration ratio in soil improved with an end-bearing stone column of  $\phi = 35^\circ$  and raised to 2.63 and 4.71 at  $\phi = 50^\circ$ , ranging from 1.41 to 2.35 for area replacement ratios of 7% and 16%.

**Keywords:** Stone column, soft clay, Stresses, PLAXIS 3D.

## 1. INTRODUCTION

A cylindrical-shaped container with a rigid outer wall symmetrically positioned around the stone column is utilized to model a unit cell physically. No lateral deformation at the unit cell's boundaries and no shear forces beyond the unit cell's boundaries are assumed in this idealization. The stress is concentrated on the column because the surrounding soil deforms differently than the stiffer column material when a load is applied to a composite foundation. Stone columns in a cohesive soil matrix have a stress concentration ratio ( $n$ ) of [1]

$$n = \frac{\sigma_c}{\sigma_s} \quad (1)$$

Where  $\sigma_c$  denotes the stress in the stone column and  $\sigma_s$  denotes the stress in the cohesive soil. The area replacement ratio is derived by dividing the column's area by the area of the soil's tributaries. The volume of soil replaced depends on the quantity of soil returned in settlement and the bearing capacity increase. The bulk of stone column applications has a 15–35 % average area replacement ratio ( $a_s$ ). The definition of  $a_s$  is as follows:

$$a_s = \frac{A_c}{A_e} = C \left( \frac{d_c}{s} \right) \quad (2)$$

where

$a_s$  = area replacement ratio

$A_c$  = cross-sectional area of the column

$A_e$  = tributary area of the column

$d_c$  = diameter of the column

$s$  = center-to-center spacing between columns in a square or equilateral triangular pattern

$C$  = constant ( $\pi/4$  or 0.785 for a square pattern or  $\pi/(2\sqrt{3})$  or 0.907 for an equilateral triangular pattern) [1].

The stress concentration ratio,  $n$ , is studied in the laboratory using 72 model tests of soft clays with undrained shear strengths,  $c_u$ , ranging from 6 to 12 kPa, when the length-to-diameter ratio of an end-bearing stone column was set to 8, the,  $n$  values, varied from 1.4 to 3.8. With ( $L/D = 6$ ),  $n$  falls between (1.2 and 3.4) in the case of floating columns. Furthermore, the  $c_u$  of cohesive soil increases to 9 and 12 kPa [2, 3]. ANSYS 18 study showed that for  $a_s = 25\%$ , the  $n$  rose from 1.0 at  $q/c_u = 3$  to 5.70 at 25.0 ( $q =$  applied load).  $n$  increases with stress ( $q/c_u > 5$ ). The maximum area ratio shows the most significant  $n$  [4]. Stone columns under embankment loading are analyzed using 2D FEA. The suggested 2D strip model matched the 3D baseline FEA results. The strip model outperforms the composite technique. The fill stress,  $q_a$ , normalizes column depth,  $z$ .  $n$  value increases from 4 at the soil's surface to 14 at ( $z/q_a = 4$ ) and remains constant [5]. A rigid-foundation floating stone column is modeled in 3D DEM. Settlement enhances shallow column porosity. The column increases radial stress in the soft clay's upper section. The stress concentration ratio drops from 2.5 to 1.55 after loading [6]. Stone column rigidity greatly affected consolidation speed in a laboratory study. Geotextile-encased stone columns showed steady-stress concentration ratios of 4–11, compared to 4–6 for normal stone columns [7]. Elastic methods exaggerate settlement improvement and should be avoided in stiff soils.

Semi-empirical predictions are more accurate for higher modular ratios (e.g.,  $E_c/E_s = 40$ ).  $E_c/E_s$  ranged from 5 to 40, and  $n$  was 2 to 3.4 [8]. Stone columns consolidated soft ground from equal load to free strain. Parametric research measured foundation stiffness. As foundation stiffness increases, soil's steady stress concentration ratio,  $n$ , is always one under free strain conditions. At equal strain loading,  $n$  is less than one, rises to 4, and stabilizes [9]. Experiments revealed that stone columns had stronger bearing capacity than sand columns. Then, for the sand column, it was 1.5, and  $n$  for the sand +11 % lime was 2. The stiffnesses of both types of columns improved by 1.7 to 5.5 and 6.5 percent, respectively [10]. The unit cell or plane strain model can calculate  $n$  for a stone column to account for this. The plane strain model's  $n$  was 1.76 to 2.93, while the unit cell model was 2.48 to 3.14. Stone column failure mechanism studies contradict the unit cell paradigm [11]. According to Plaxis 2D numerical computations, rigid foundations have a stress concentration ratio of 2.5 to 5.0, while flexible foundations have 1.8–3.0. Soft clay's elasticity modulus decreases the stress concentration ratio [12]. The unit cell's one-dimensional loading within the soft soils' over-consolidated stress range represents stress dispersion. Well-graded angular particles increase the stress concentration ratio. At 40 and 52 kPa pressures, the stress concentration ratio,  $n$ , varied from 2-7 to 2-5 after 180 hours [13].  $n$  decreases when the bearing capacity ratio to total stress increases. Four triangular stone columns have a higher  $n$  than four square columns. Six columns did the same. Model experiments showed that  $n$  at steady-state varies from 2 for a single column to 4.6 for a six-column structure [14]. The simplified approach and numerical research agree when the steady-stress concentration ratio is 2–6. This method showed that applied loads increased the steady-stress concentration ratio [15]. According to parametric research, the stress concentration factor develops from 4.0 to 4.63 for spacing-to-diameter ratios of 2 and 5, respectively [16].

This study investigated the stability of a single stone column using a soft clay layer over stiff soil and a rigid foundation. In terms of stress distribution, individual stone columns floating in the same soil conditions were also compared to nearby soil. After soil improvement, the stress concentrations on the columns and adjacent soil were measured.

## 2. 3D MODELLING APPROACH

The numerical modeling was performed using Plaxis 3D 2020. All soil layers were modeled using the elastic, completely plastic Mohr-Coulomb model. The soil layer parameter was determined using borehole data near the plate load test site; values are listed in Table 1. The model of the stone column is used in three different diameters (0.8, 1, and 1.2 m). The 10 m long stone column is utilized in two circumstances, a floating column and an end-bearing column, with (L/D) ranging from 8.33 to 12.5 for all numerical models. The thickness of the clay layer was considered to extend five meters after the end of the column in the floating condition, whereas it is equal to the length of the column in the column with end bearing column, as illustrated in Figure 1, so the (L/D) ranging from 8.33 to 12.5 for all numerical models. It was assumed that the clay soil was entirely saturated, and the influence of pore water pressure was ignored because the experiments were fast and undrained, and the relationship did not depend on time. A circular precast concrete footing with a diameter of 3 m that is elastic and impervious to water was simulated. Due to the high permeability of crushed stone, the stone column was modeled using the Mohr-Coulomb method. The stress concentrations on the columns and adjoining soil following soil improvement were determined using a single-end bearing stone column supported by a circular rigid foundation supported by a soft clay layer on a stiff layer. The stress distributions of individual stone columns floating in the same soil conditions as the surrounding soil were compared. The unimproved rigid foundation loads must be studied first to regulate the improvement in rigid foundation loads after stone column installation in soft soils. The stress distribution at the stone column tops is compared to the unimproved stress distribution to determine the stress concentration ratio.

Table 1. Material properties employed in the analysis.

Properties	Units	Materials									
		Stone column			Soft Soil						Raft Foundation
		Mohr-Coulomb			Mohr-Coulomb						Linear-Isotropic
$\gamma_{unsat}$	kN/m <sup>3</sup>	16.3	16.3	16.3	13.52	14.11	14.72	15.14	15.65	16.23	25.0
$\gamma_{sat}$	kN/m <sup>3</sup>				17.32	17.83	19.11	19.22	19.56	19.73	-
E	kN/m <sup>2</sup>	45000	50000	56000	1973	2415	3300	4025	5500	7100	60000
$\nu$	-	0.30	0.30	0.30	0.40	0.40	0.40	0.40	0.40	0.40	0.15
$c_u$	kN/m <sup>2</sup>	0	0	0	6	9	15	20	30	40	0
$\phi$	degree	35	42	50	0	0	0	0	0	0	0
$\psi$	degree	0			0	0	0	0	0	0	0

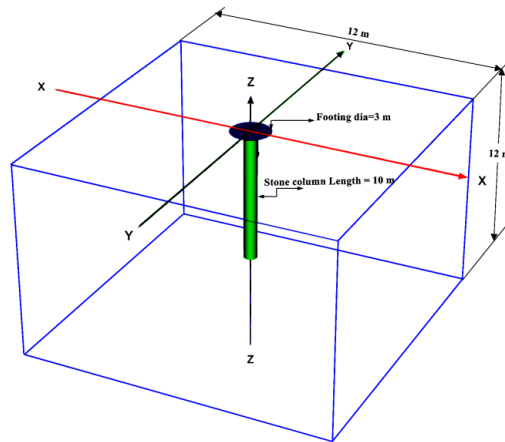


Figure 1: Geometry of the model.

The elasticity modulus, the length of the stone column, and the area replacement ratio are all varied in this parametric study to determine the effect of each parameter. The stiffness of the stone column is constant at three different substitution area ratios and six different elasticity values for soft. The column's modulus of elasticity is changed twice to account for the same weak soil modulus of elasticity and the precise replacement area ratio values. Each set of stiff foundation analyses contained 18 columns. The maximum pressure on the foundation is indicated at a 10% decrease in diameter.

### 3. RESULTS AND DISCUSSION

A total of 114 numerical models were completed using (Plaxis 3D 2020), six of which were for cohesive soils only, with undrained shear strengths ranging from 6 to 40 kPa, and 36 models for soil treated with stone columns, each of which had a friction angle,  $\phi = 35^\circ$  and three different diameters, 0.8 m, 1 m, and 1.2 m, respectively, or with area replacement ratios ranging from 7 to 16 %. The same 36 models are replicated twice, once for columns with  $\phi = 42^\circ$  and once for columns with  $\phi = 50^\circ$ , using the same method each time. The relationship between the stress concentration ratio and cohesion of soft clay,  $c_u$  soils improved with stone columns with  $\phi = 35^\circ$  a variable replacement area is depicted in Figure 2. (7, 11, and 16%). The stone column was employed in two distinct ways: floating and end-bearing columns. As illustrated in the graph, the  $n$  is significantly affected by changes in the soil's  $c_u$ , as  $n$  decreases as  $c_u$  increases for all soil types and in end-bearing and floating scenarios.

As an illustration, the  $n$  values were (2.83, 2.41, 2.07, 1.88, 1.75, and 1.74) for the end-bearing stone column treated soil with 7% replacement area for ( $c_u = 6, 9, 15, 20, 30,$  and  $40$  kPa), indicating that the effect of using this technique is active in the case of medium or stiff cohesive soils, in addition, a result of the increased hardness of the soil column's and the soil's composite substance, where the column bears the majority of the load. Additionally, it was noted that when the floating column is used, the previous values of  $n$  become (2.26, 1.81, 1.57, 1.34, 1.18, and 1.14) for the same values of  $c_u$  and the exact replacement area, which is due to the stone column's increased bearing capacity as a result of its stability on solid soil. This aligns with the determinations of many investigators, such as [16], who found that when ( $L/D = 10$ ) was used for floating and end-bearing stone columns, the values of  $n$  were 3.31 and 4.92, respectively. Additionally, a substantial alteration in the  $n$  value was detected when the ratio of the area replaced was changed. The  $n$  value decreased as the  $c_u$  increased for both types of stone columns and all value of  $c_u$ . Where  $n$  was 2.07 at  $as = 7\%$  for soil with  $c_u = 15$  kPa treated with end-bearing column and declined to 1.38 at  $as = 16\%$ . It can be noticed that the alteration between the values of  $n$  becomes negligible when the stress concentration ratio,  $c_u$ , increases from 20 to 40 kPa.

Changing the friction angle of the stone column in the case of floating columns has no effect on the values of the stress concentration ratio,  $n$ , for all values of  $c_u$ , even when the ratio of the replaced area is changed for all values of  $c_u$  of soft clay, as illustrated in Figure 3. However, in the case of the end-bearing column, the value of  $n$  has increased by 36%. When equivalent values of  $c_u$  are used, it is possible to see that the value of  $n$  at  $as$  has decreased to (3.41, 20.4, 2.21, 2.45, 28.9, 3.41). This is because adhesion is principally responsible for determining the carrying capacity of floating columns between the stone column and the neighboring soil, or in other words, the  $c_u$  values. In comparison, the end bearing column's carrying capacity is specified by the base bearing, which is controlled by the column and the stiffeners of the layer upon which it is placed. This is supported by other researchers in experimental and statistical works [18, 1, and 3].

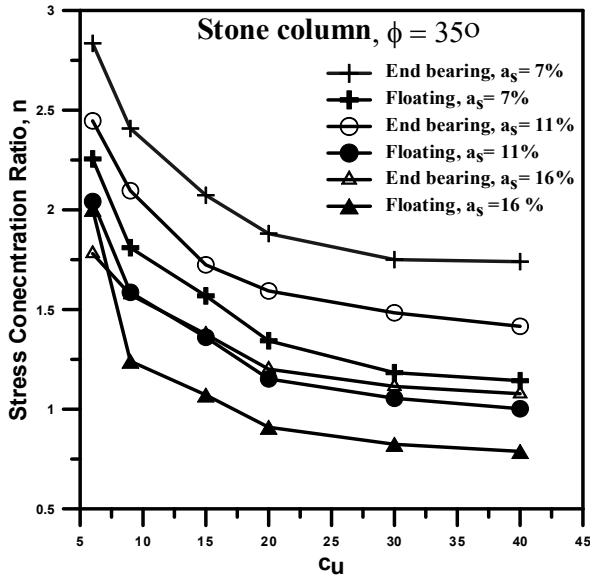


Figure 2:  $n$  versus  $c_u$  for the stone column, ( $\phi = 35^\circ$ ).

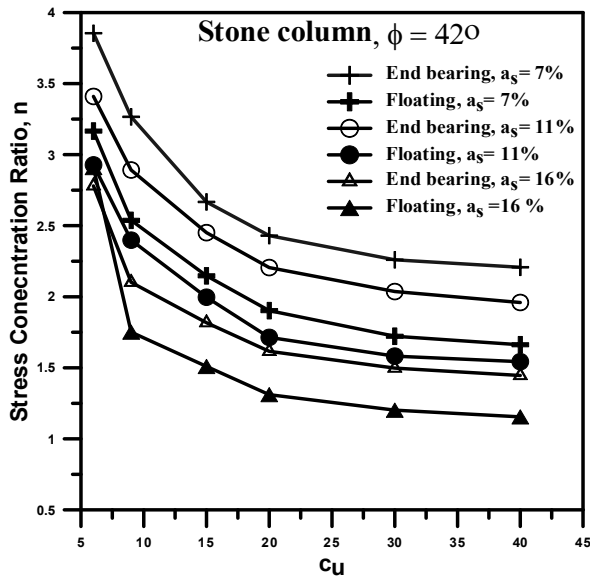


Figure 3: Stress concentration ratio versus  $c_u$  for the stone column with ( $\phi = 42^\circ$ ).

The use of crushed stone  $\phi = 50^\circ$  improves the load concentration ratio in both types of columns and for all diameters of the stone column and all values of  $c_u$  for the soft soil near the column, nevertheless for the kind of column. However, floating columns significantly impact the column's load share to twice that of the column of  $\phi = 35^\circ$ . Compared to the initial configuration, the stone column's load share has increased by 42%. As shown in Fig. 3, for the soft soils enhanced with the floating stone columns with ( $c_u = 6, 9, 15, 20, 30, \text{ and } 40$  kPa), the average values of  $n$  were (5.31, 4.49, 3.78, 3.33, 3.16, 3.03). For example, while altering  $c_u$  from 6 kPa to 40 kPa and utilizing the bearing columns of load at the ratio as the average of  $n$  is 3.85, it drops to 3.57 when  $a_s = 11\%$  and then drops even further to 2.75 when  $a_s = 16\%$ . Figure 4 shows that the  $n$  values increased by only a tiny amount, which is about 16%, when converting from the floating to end load columns. This is mainly due to the noticeable increase in the column's stiffness, resulting in lower baseload participation averages.

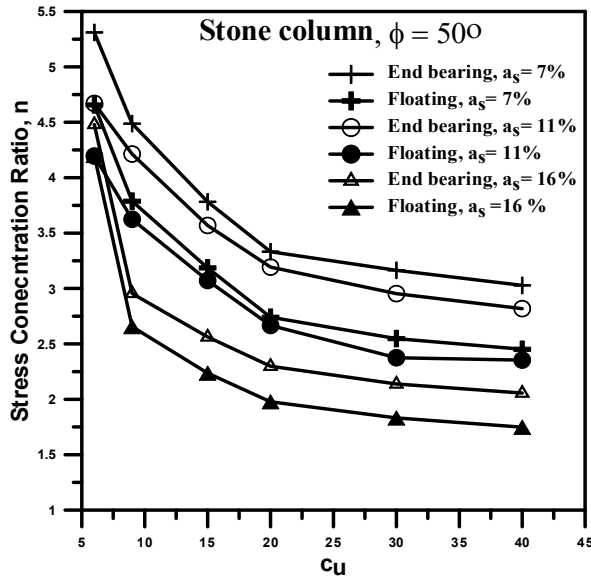


Figure 4:  $n$  versus  $c_u$  for the stone column ( $\phi = 50^\circ$ ).

Table 2 and Figure 5 shows that the average  $n$  attained its highest value of 4.71 when the end bearing column was used, and the friction angle of the material of the stone column  $\phi = 50^\circ$  for the soil improved with  $c_u = 6$  kPa. When soil with cohesion of  $40^\circ$  was treated with a single column of  $\phi = 35^\circ$ , the lowest average  $n$  was attained, and this value is comparable to that of the enhanced soil at  $c_u = 30$  kPa. With these  $c_u$  values, using this soil improvement method is not practical and represents an uneconomical solution, as is evident if the column's angle of friction is medium; therefore, it is not suggested in this situation. This can be explained by the soil's ( $E_s$ ) and stone column's ( $E_c$ ); the amount of stress concentration will be more significant if the stiffness of a stone column is higher than that of the surrounding soil, as stated by [19, 20] who they also found, that the  $n$ , typically ranges from 3 to 4. However, if the stiffness of the stone column increases, the values of  $n$  rise sharply, particularly here in the stone column of end bearing, and reach a peak, as seen above, in the end bearing stone column with  $\phi = 50^\circ$  for soil with  $c_u = 40$  kPa, where  $n = 2.36$ . This value justifies using this technology to improve the qualities of weak soils while staying within established parameters. As previously stated, the end-bearing columns have higher  $n$  values than the floating columns, aside from the most significant finding: this procedure is highly effective in fragile soils. At the same time, the results of the experiments showed that floating stone columns could be used to improve the ultimate bearing capacity of soft soil despite the modest area replacement ratio [21-24].

Table 2: Average Stress Concentration Ratio Values.

$c_u$ [kPa]	$\phi = 35^\circ$		$\phi = 42^\circ$		$\phi = 50^\circ$	
	Floating	End	Floating	End	Floating	End
6	1.95	2.35	2.95	3.35	4.37	4.71
9	1.55	2.03	2.27	2.75	3.36	3.89
15	1.33	1.72	1.88	2.31	2.83	3.30
20	1.13	1.56	1.64	2.08	2.46	2.94
30	1.02	1.45	1.50	1.93	2.25	2.75
40	1	1.41	1.45	1.87	2.18	2.63

An elastic modulus ratio ( $E_c/E_s$ ), which indicates a stone column's elastic modulus, is shown in Figure 6 as a function of the stress concentration ratio,  $n$ . The stiffness ratio affects the stress concentration ratio, particularly in the end-bearing columns. As the cohesion changes from ( $c_u = 6$  kPa) to ( $c_u = 40$  kPa), the stiffness ratio changes from 6.34 to 22.81 when the soil is improved with columns at an angle of friction ( $\phi = 35^\circ$ ). At the same time, the ( $E_c/E_s$ ) ratio increases at columns of ( $\phi = 42^\circ$ ) to reach 25.34 and then ( $E_c/E_s = 28.38$ ) when columns of ( $\phi = 50^\circ$ ) are utilized (2.1, 3, and 4.37) for the class bars and (2.3, 3.35, 4.71) for the end bearing are their maximum  $n$  for the stiffness ratio's initial highest values. In contrast, the stiffness ratio of a stone column to a soft clay column is 10 to 20 in most cases [25]. The stress concentration ratio,  $n$  is close to one in columns with ( $E_c/E_s$ ) values of around 6 in stone columns of the ( $\phi = 35^\circ$ ), while  $n$  climbs for almost

the same proportion in the columns with ( $\phi = 50^\circ$ ) to reach two and for the end bearing columns, it is between 1.5 and 2.5 [25]. The current behavior is consistent with [3].

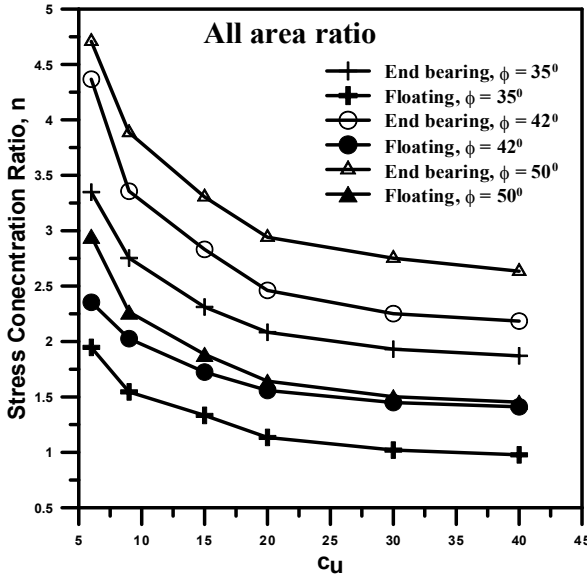


Figure 5: Stress concentration ratio,  $n$  versus  $C_u$  for all area replacement ratio,  $a_s$ .

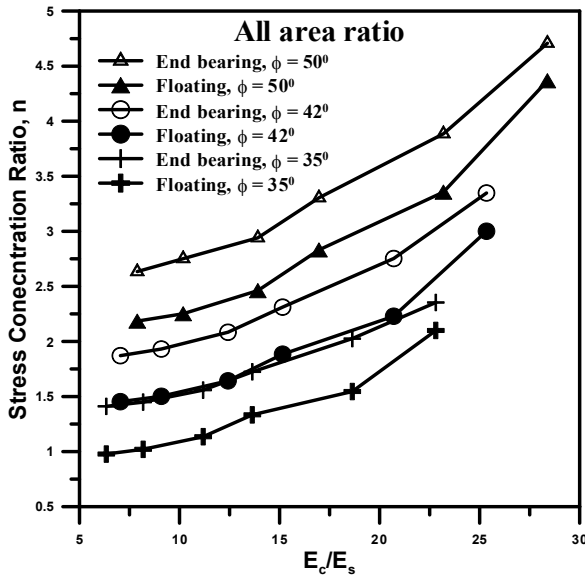


Figure 6: Stress concentration ratio,  $n$  versus  $(E_c/E_s)$  for all area replacement ratio,  $a_s$ .

#### 4. CONCLUSIONS

The soil's undrained shear strength was altered from 6 to 40 kPa, and the stone column's diameter was changed as well, resulting in a variation in the replacement ratio for the improved area of 7 to 16 percent. This study's primary findings were as follows once it had finished its assignment:

- It is achievable to have a stress concentration ratio of 1 to 4,71.
- A lower area replacement ratio and soft clay soil raise the value of  $n$ .

- The value of  $n$  drops when utilizing floating stone columns, and their use is illogical and inefficient when the  $c_u$  value reaches 40 kPa.
- An evolution in the stone column's friction angle has a noticeable effect on the value of  $n$ , reaching its highest value in columns with  $f = 50$ .
- When  $c_u$  is increased from 20 kPa to 40 kPa, the  $n$  values are close together.
- $n$  reaches its maximum value at a hardness ratio of ( $E_c/E_s = 28$ ) when the hardness ratio is at its highest point

## REFERENCES

- [1] Han J. Principles and practice of ground improvement. John Wiley & Sons; 2015 Jun 22.
- [2] Fattah MY, Shlash KT, Al-Waily MJ. Stress concentration ratio of model stone columns in soft clays. *Geotechnical Testing Journal*. 2011 Jan 1;34(1):1.
- [3] Al-Waily MJ, Fattah MY, Al-Qaisi MS. Experimental and Statistical Study on Single and Groups of Stone Columns. In *Key Engineering Materials 2020* (Vol. 857, pp. 399-408). Trans Tech Publications Ltd.
- [4] Ahmed A. A, Fattah M. Y. Distribution of Stresses Below Footings Supported by Stone Columns. *Journal of Engineering Science and Technology*. 2021 Apr;16(2):1719-32.
- [5] Vahedian A, Mahini SS, Aghdai SA. A Short State-of-the-Art Review on Construction and Settlement of Soft Clay Soil Reinforced with Stone Column. *International Journal of Engineering and Technology*. 2014.
- [6] Liu F, Guo P, Hu H, Zhu C, Gong X. Loading Behavior and Soil-Structure Interaction for a Floating Stone Column under Rigid Foundation: A DEM Study. *Geofluids*. 2021 Sep 21;2021.
- [7] Abdulrasool G. Effect of Column Stiffness on Consolidation Behavior of Stone Column-Treated Clay (Doctoral dissertation, University of Kansas). 2016.
- [8] Sexton BG, McCabe BA, Castro J. Appraising stone column settlement prediction methods using finite element analyses. *Acta Geotechnica*. 2014 Dec;9(6):993-1011.
- [9] Tai P, Indraratna B, Rujikiatkamjorn C. Consolidation Analysis of Soft Ground Improved by Stone Columns Incorporating Foundation Stiffness. *International Journal of Geomechanics*. 2020 Jun 1;20(6):04020067.
- [10] Al-Gharbawi AS, Rajab NA. Comparison between sand columns and sand columns stabilized with lime or cement with stone columns embedded in soft soil. *Engineering and Technology Journal*. 2016 Dec 28;34(15):2805-15.
- [11] Gaber M, Kasa A, Rahman NA, Alsharaf JM. Comparison between unit cell and plane strain models of stone column ground improvement. *International Journal of Engineering & Technology*. 2018;7(2):263-9.
- [12] Gaber M, Kasa A, Rahman NA, Alsharaf JM. Comparison between unit cell and plane strain models of stone column ground improvement. *International Journal of Engineering & Technology*. 2018;7(2):263-9.
- [13] Siahaan F, Indraratna B, Rujikiatkamjorn C, Basack S. Vertical stresses in stone column and soft clay during one-dimensional consolidation test. 2014.
- [14] Paul J, Sindhu AR. Study on stress concentration ratio of stone column reinforced soft clay. *International Research Journal of Engineering and Technology (IRJET)*. 2018;5(4):3535-9.
- [15] Han J, Ye SL. A theoretical solution for consolidation rates of stone column-reinforced foundations accounting for smear and well resistance effects. *International Journal of Geomechanics*. 2002 Apr;2(2):135-51.
- [16] Sakr M, Shahin M, Farouk A, Moneim K. Numerical Modeling of Stone Columns in Soft Clay for Drained and Undrained Conditions. *Electronic Journal of Geotechnical Engineering*. 2017;22(6):1907-24.
- [17] Al-Auqbi ST, Salim NM, Mahmood MR. The Impact of Using Different Types of Soft Soils Treated by Stone Columns on Creep Behavior. In *IOP Conference Series: Earth and Environmental Science 2022* (Vol. 961, No. 1, p. 012052). IOP Publishing.
- [18] Al-Waily MJ. Stress concentration ratio of model stone columns improved by additives (Doctoral dissertation, Ph. D. Thesis, University of Technology, Building and Construction Engineering Department).2007
- [19] Goughnour RR, AA B. Analysis of stone column-soil matrix interaction under vertical load. 1979
- [20] Aboshi H. The composer, a method to improve characteristics of soft clays by inclusion of large diameter sand columns. In *Proc. of 1st Int. Conf. on Soil Reinforcement 1979* (Vol. 1, pp. 211-216).
- [21] Karkush M, Jabbar A. An Improvement of Bearing Capacity of Soft Soil and Reducing Excess Porewater Pressure Using Several Patterns of Floating Stone Columns. *Journal of Engineering Research*. 2021 Oct 20.
- [22] Karkush MO, Jabbar A. Improvement of soft soil using linear distributed floating stone columns under foundation subjected to static and cyclic loading. *Civil Engineering Journal*. 2019 Mar 19;5(3):702-11.
- [23] Karkush M, Jabbar A. Behavior of floating stone columns and development of porewater pressure under cyclic loading. *Transportation Infrastructure Geotechnology*. 2022 Apr;9(2):236-49.

- [24] Karkush M, Jabbar A. An Effect of several patterns of floating stone columns on the bearing capacity and porewater pressure in saturated soft soil. *Journal of Engineering Research*. 2022;10(2B):84-97.
- [25] Poon B, Chan K. Stress concentration ratio and design method for stone columns using 2D FEA with equivalent strips. In *Proceedings of the 18th International Conference on Soil Mechanics and Geotechnical Engineering 2013* (pp. 2585-2588).